

Paper submitted to the Journal: Numerical Heat Transfer B

ON THE TRULY MESHLESS SOLUTION OF HEAT CONDUCTION PROBLEMS IN HETEROGENEOUS MEDIA

Jiannong Fang ^{a,*}, Gao-Feng Zhao ^b, Jian Zhao ^b, Aurèle Parriaux ^a

^a *Ecole Polytechnique Fédérale de Lausanne (EPFL), Engineering and
Environmental Geology Laboratory, ENAC-ICARE-GEOLEP, Station 18, CH-1015
Lausanne, Switzerland*

^b *Ecole Polytechnique Fédérale de Lausanne (EPFL), Rock Mechanics Laboratory,
ENAC-ICARE-LMR, Station 18, CH-1015 Lausanne, Switzerland*

07 October 2008

(Revised)

Abbreviated title: TRULY MESHLESS HEAT CONDUCTION

* Address correspondence to Jiannong Fang, Ecole Polytechnique Fédérale de Lausanne, ENAC-ICARE-GEOLEP, Station 18, CH-1015 Lausanne, Switzerland.
E-mail: jiannong.fang@epfl.ch

Abstract

A truly meshless method based on the Weighted Least Squares (WLS) approximation and the method of point collocation is proposed to solve heat conduction problems in heterogeneous media. It is shown that, in case of strong heterogeneity, accurate and smooth solutions for temperature and heat flux can be obtained by applying the WLS approximation in each homogeneous domain and using a double stage WLS approximation technique together with a proper neighbor selection criterion at each interface.

NOMENCLATURE

a	vector of unknowns	P	vector of monomials
A	matrix of computation	q	normal heat flux
b	vector of function differences	Q^x, Q^y	components of heat flux vector
C	matrix of computation	s	heat source
e	vector of truncation errors	T	Temperature
f	scalar field	x	position vector
G	matrix of final algebra equations	x, y	Cartesian coordinates
h	searching radius	w	weight function
m	number of neighbor points	κ	thermal conductivity
M	matrix of computation	Subscripts	
n	normal coordinate	i, j, k, n	point index
N	number of total points	α, β	component index

1. Introduction

In recent years, a large family of meshless methods with the aim of getting rid of mesh constraints has been developed for solving partial differential equations. The basic idea of meshless methods is to provide numerical solutions on a set of arbitrarily distributed points without using any mesh to connect them. Compared to mesh generation, it is relatively simple to establish a point distribution and adapt it locally. The points are grouped together in “clouds” where a local approximation for the problem variables is written. Depending on the methodology used to discretize the equations, meshless methods can be classified into two major categories: meshless strong-form methods and Meshless weak-form methods. Most of meshless weak-form methods such as the element free Galerkin method [1] are “meshless” only in terms of the numerical approximation of field variables and they have to use a background mesh to do numerical integration of a weak form over the problem domain, which is computationally expensive. Meshless strong-form methods such as the generalized finite difference method [2] often use the point collocation method to satisfy governing partial differential equations and boundary conditions. They are simple to implement and computationally efficient. Since they do not need any background mesh, they are truly meshless methods.

Finite point method (FPM) is a truly meshless method proposed by Oñate *et al.* [3]. FPM uses the weighted least squares (WLS) approximation within each point cloud, which can be easily constructed to have consistency of a desired order, and adopts the point collocation method to obtain discrete equations directly from partial differential equations. Therefore, it is easy for numerical implementation and boundary conditions can be implemented in a natural way by just prescribing boundary conditions on points placed on boundaries. We noted that the finite point method is similar to the weighted least squares collocation method proposed by Sadat and Prax [4] for solving fluid flow and heat transfer problems. FPM has been applied and extended successfully to solve a range of problems including convective-diffusive transport [5], compressible flow [6], incompressible flow [7, 8], potential flow [9],

metal solidification [10], elasticity problems in structural mechanics [11], two-phase flows [12], and fluid-structure interactions [13]. Although quite successful in many applications, the extension and validation of FPM for problems involving heterogeneous media remains a big challenge [11]. Sadat *et al.* [14] attempted to solve a heterogeneous heat conduction problem in a two-layer wall by using the weighted least squares collocation method and found that one has to use a double stage WLS approximation technique in which a second order numerical derivation is obtained from a sequence of two first order numerical derivations by WLS and take into account the neighbors of each neighbor of the calculation node in order to achieve sufficient accuracy in the case of strong heterogeneity.

The authors revisited the method of Sadat *et al.* [14] for heterogeneous heat conduction problems and found that fluctuations existed in the predicted results of temperature and heat flux in the case of strong heterogeneity. In this paper we will report this finding and show that accurate and smooth solutions for temperature and heat flux can be obtained by applying the usual WLS approximation technique in each homogeneous domain and using the double stage WLS approximation technique together with a proper neighbor selection criterion at each interface.

The paper is organized as follows. In section 2 the weighted least squares approximation method is briefly described. Then, the double stage WLS approximation technique and the proposed method for solving heat conduction problems in heterogeneous media are presented. There numerical examples are considered in section 4 for the purpose of evaluating accuracy of different methods. The paper ends up with concluding remarks in section 5.

2. The weighted least squares method

The weighted least squares (WLS) method gives an approximation of a function $f(\mathbf{x})$ and its derivatives at a given point \mathbf{x} by using only the discrete function values at the neighbor points being in the support domain of \mathbf{x} (usually a ball in 3D or a disk in 2D). An advantage of this method is that it does not require regular

distribution of points. In the following, we briefly explain the method in 2D (extension to 3D is straightforward).

Consider a Taylor's expansion of $f(\mathbf{x}_i)$ around \mathbf{x}

$$f(\mathbf{x}_i) = f(\mathbf{x}) + \sum_{\alpha=1}^2 f_{\alpha}(\mathbf{x})(x_{i\alpha} - x_{\alpha}) + \frac{1}{2} \sum_{\alpha,\beta=1}^2 f_{\alpha\beta}(\mathbf{x})(x_{i\alpha} - x_{\alpha})(x_{i\beta} - x_{\beta}) + e_i, \quad (1)$$

where e_i is the truncation error in the Taylor's series expansion (here only to second-order, higher order expansions are, of course, possible), f_{α} is the derivative with respect to x_{α} (the α -th component of the position vector \mathbf{x}) and $f_{\alpha\beta}$ the derivative with respect to x_{α} and x_{β} . The symbols $x_{i\alpha}$ and $x_{i\beta}$ denote the α -th and β -th components of the position vector \mathbf{x}_i respectively. From the given function values $f(\mathbf{x})$ and $f(\mathbf{x}_i)$ ($i=1,2,\dots,m$), the unknowns f_{α} and $f_{\alpha\beta}$ for $\alpha,\beta=1,2$ (note that $f_{\alpha\beta} = f_{\beta\alpha}$) are computed by minimizing the error e_i for $i=1,2,\dots,m$. Here m is the number of neighbor points inside the support domain of \mathbf{x} .

Using the Taylor's expansion (1) repeatedly for $i=1,2,\dots,m$, the system of equations for the five unknowns can be written as

$$\mathbf{e} = \mathbf{M}\mathbf{a} - \mathbf{b} \quad (2)$$

With

$$\mathbf{e} = [e_1, e_2, \dots, e_m]^T,$$

$$\mathbf{a} = [f_1, f_2, f_{11}, f_{12}, f_{22}]^T,$$

$$\mathbf{b} = [f(\mathbf{x}_1) - f(\mathbf{x}), f(\mathbf{x}_2) - f(\mathbf{x}), \dots, f(\mathbf{x}_m) - f(\mathbf{x})]^T,$$

$$\mathbf{M} = [\mathbf{p}_1, \mathbf{p}_2, \dots, \mathbf{p}_m]^T$$

where \mathbf{a} is the vector containing the five unknowns and \mathbf{M} is a matrix in which the vector \mathbf{p}_i is defined as

$$\mathbf{p}_i = \left[x_{i1} - x_1, x_{i2} - x_2, \frac{(x_{i1} - x_1)^2}{2}, (x_{i1} - x_1)(x_{i2} - x_2), \frac{(x_{i2} - x_2)^2}{2} \right]^T \quad (3)$$

For $m > 5$, this system is over-determined with respect to the five unknowns in \mathbf{a} . This problem can be simply overcome by determining the unknown vector \mathbf{a} by minimizing the quadratic form

$$J = \sum_{i=1}^m w_i e_i^2 \quad (4)$$

where $w_i = w(\mathbf{x}_i - \mathbf{x})$ is the value of a weight function w at point \mathbf{x}_i . Standard minimization of J with respect to \mathbf{a} gives

$$\mathbf{a} = \mathbf{C}^{-1} \mathbf{A} \mathbf{b} \quad (5)$$

Where

$$\mathbf{C} = \sum_{i=1}^m w_i \mathbf{p}_i \mathbf{p}_i^T, \quad (6)$$

$$\mathbf{A} = [w_1 \mathbf{p}_1, w_2 \mathbf{p}_2, \dots, w_m \mathbf{p}_m]. \quad (7)$$

In this paper, we use a Gaussian weight function of the following form

$$w(r, h) = \begin{cases} \exp(-\varepsilon r^2 / h^2), & \text{if } r \leq h; \\ 0, & \text{else,} \end{cases} \quad (8)$$

where $r = \|\mathbf{x}_i - \mathbf{x}\|$ and ε is a positive constant chosen to be equal to 6.3 in our computations. The size of the searching radius h determines m , the number of neighboring points around \mathbf{x} to be used for WLS approximation.

3. Steady heat conduction in a heterogeneous medium and numerical methods

Two-dimensional steady heat conduction in a heterogeneous medium is governed by the Laplace equation as follows:

$$\frac{\partial}{\partial x} \left(\kappa \frac{\partial T}{\partial x} \right) + \frac{\partial}{\partial y} \left(\kappa \frac{\partial T}{\partial y} \right) = s \quad (9)$$

where T is the temperature, κ is the thermal conductivity of the medium, and s is the source term. On the boundaries, Dirichlet boundary condition

$$T - T_b = 0 \quad \text{on } \Gamma_d \quad (10)$$

and Neumann boundary condition

$$\kappa \frac{\partial T}{\partial n} - q = 0 \quad \text{on } \Gamma_n \quad (11)$$

are to be satisfied with the prescribed values of the temperature T_b and the normal heat flux q .

To obtain the discretized equations, the *point collocation* method is applied, i.e., the Laplace equation (9) and the boundary conditions (10)-(11) are forced to be satisfied at each internal and boundary point respectively. This gives the set of equations

$$[L]_i = \left[\frac{\partial}{\partial x} \left(\kappa \frac{\partial T}{\partial x} \right) \right]_i + \left[\frac{\partial}{\partial y} \left(\kappa \frac{\partial T}{\partial y} \right) \right]_i - s_i = 0 \quad \text{in } \Omega \quad (12)$$

$$T_j - T_b^j = 0 \quad \text{on } \Gamma_d \quad (13)$$

$$\left[\kappa \frac{\partial T}{\partial n} \right]_k - q_k = 0 \quad \text{on } \Gamma_n \quad (14)$$

Expressing spatial derivatives occurred in the above set of equations in terms of the unknown temperatures at points by the WLS method leads to the final discretized system of equations

$$\mathbf{G}\tilde{\mathbf{h}} = \tilde{\mathbf{f}}, \quad (15)$$

where \mathbf{G} is the coefficient matrix, vector $\tilde{\mathbf{h}}$ contains the unknown temperatures and $\tilde{\mathbf{f}}$ is a vector containing the contributions from the prescribed values s_i , T_b^j and q_k .

How to express the two derivative terms in $[L]_i$ in terms of the unknown temperatures is an important issue. Take the first term as example, it can be expanded as

$$\left[\frac{\partial}{\partial x} \left(\kappa \frac{\partial T}{\partial x} \right) \right]_i = \left[\kappa \frac{\partial^2 T}{\partial x^2} \right]_i + \left[\frac{\partial \kappa}{\partial x} \right]_i \left[\frac{\partial T}{\partial x} \right]_i \quad (16)$$

Therefore, a natural way is to calculate the first derivative of κ by WLS and express the other derivatives in terms of the unknown temperatures by WLS again. However, it was shown [14] that this formulation implies important errors that increase with the degree of heterogeneity. Hence, it will be excluded from our consideration. Sadat *et al.* [14] proposed another way by first representing the heat flux at each point in terms of temperatures using WLS and then, based on these heat flux expressions, using the WLS approximation again for the first derivatives of the heat flux. Because this approximation procedure uses WLS twice in a sequence, we denominate it as the double stage WLS approximation. The detailed implementation of the method is described below.

Take again the first term in $[L]_i$ as example, it can be expressed as

$$\left[\frac{\partial}{\partial x} \left(\kappa \frac{\partial T}{\partial x} \right) \right]_i = \sum_{j=1}^N a_{ij} Q_j^x \quad (17)$$

where

$$Q_j^x = \left[\kappa \frac{\partial T}{\partial x} \right]_j \quad (18)$$

and a_{ij} are the coefficients in the WLS approximation of the first derivative with respect to x at point i . Here N is the total number of points. Note that only the coefficients corresponding to the neighboring points of i are nonzero. The term Q_j^x is determined by

$$Q_j^x = \kappa_j \sum_{n=1}^N a_{jn} T_n \quad (19)$$

where κ_j corresponds to the thermal conductivity at point j and a_{jn} are the coefficients in the WLS approximation of the first derivative with respect to x at point j . The discretization of the first term in $[L]_i$ is finally written as

$$\sum_{j=1}^N \sum_{n=1}^N \kappa_j a_{ij} a_{jn} T_n \quad (20)$$

This expression takes into account the neighbors of the neighbors of the point

considered. For a point on the interface separating two domains of different thermal conductivities, Sadat *et al.* [14] suggested that its thermal conductivity can be taken from one of the two domains. However, in the next section, we will show that different choice of thermal conductivity gives different results.

From our numerical tests, we found that the method of Sadat *et al.* using the double stage WLS approximation described above yields much improved results. However, the simulated results exhibited prominent fluctuations in both temperature and heat flux. One reason is that, in heterogeneous heat conduction problems, the first derivatives of the temperature are discontinuous at the interface separating two domains of different thermal conductivities, so the WLS approximation of the first derivatives of the temperature for the points near the interface introduces large errors when the neighboring points are chosen as usual from both domains. A proper neighbor selection criterion was proposed to solve the problem. That is, for a given point, it only selects its neighboring points from those who have the same thermal conductivity and those who locate on the interface. This criterion is only applied at the first stage where the first derivatives of the temperature are approximated by WLS. Although introducing the criterion into the method of Sadat *et al.* improved the results in one-dimensional problems, it still produced fluctuations in the results of two-dimensional problems. To remove the fluctuations completely, we propose a new method as follows. For a point belongs to a homogeneous domain, Eq. (12) can be simplified as

$$[L]_i = \kappa \left[\frac{\partial^2 T}{\partial x^2} + \frac{\partial^2 T}{\partial y^2} \right]_i - s_i = 0. \quad (21)$$

The second-order derivatives in Eq. (21) are approximated by WLS together with the proper neighbor selection criterion introduced above. For a point on the interface, the double stage WLS approximation is used to discretize Eq. (12). Again, to calculate heat fluxes at the first stage, the proper neighbor selection criterion is applied. Heat flux calculated on an *interface point* can have different value corresponding to different choice of the thermal conductivity value for that point. In order to obtain unique solution, the averaged heat flux is adopted in the proposed method.

Hereafter, we will call the meshless point collocation method proposed by Sadat *et al.* [14] as MPCM1 and the new method proposed in this paper as MPCM2.

4. Numerical tests

To evaluate the two methods MPCM1 and MPCM2, a steady state heat conduction problem in a two-layered composite wall, as depicted in Figure 1, is first solved in this section. This test problem was proposed by Sadat *et al.* [14] to validate their method, i.e., MPCM1 here. The two layers have the same thickness but different conductivities as κ_1 and κ_2 respectively. The ratio of conductivity κ_1/κ_2 accounts for the degree of heterogeneity of the wall. Prescribed temperatures are imposed on the two vertical surfaces, whereas the horizontal boundaries are assumed to be adiabatic. The computational domain was considered to be a square with the dimensionless length of 1. A total of 441 (21×21) points were first evenly placed in equal distance ($\Delta x = \Delta y = 0.05$) over the problem domain with 80 of them located right on the four sides of the square (21 on each side), which are so called *boundary points*, and 21 of them located right on the interface between the two layers, which are so called *interface points*. Then, the positions of boundary and interface points were fixed, while the positions of other points were shifted randomly to give an irregular point distribution, as shown in Figure 2. The searching radius h was set to $2.1\Delta x$. Both the case with a source term ($s \neq 0$) and the one without it ($s = 0$) are considered. The stationary temperature and heat flux profiles along the x-direction obtained by MPCM1 and MPCM2 are compared to the exact analytical solutions. The parameter values and the results are given in dimensionless form.

[Insert Fig. 1 here]

[Insert Fig. 2 here]

Figure 3 and Figure 4 show the results of temperature and heat flux for $\kappa_1/\kappa_2 = 0.01$ with $s = 0$ and κ_2 fixed to 1. It can be seen that MPCM1 provides acceptable results for the heat conduction problem in case of strong heterogeneity.

Nevertheless, the results predicted by MPCM1, especially the heat flux results, exhibit prominent fluctuations, as evidenced in Figure 4. Moreover, the results of MPCM1 are sensitive to the choice of the thermal conductivities on the interface points. These problems are solved perfectly by MPCM2 and the results obtained by MPCM2 match the exact solutions accurately. In Figure 5 and Figure 6, we show the results obtained by MPCM1 using the same parameters but a finer and regular grid of 1681 (41×41) points. Oscillations are still observed, but become smaller.

[Insert Fig. 3 here]

[Insert Fig. 4 here]

[Insert Fig. 5 here]

[Insert Fig. 6 here]

For the case of $s = -10$, the results with $\kappa_1/\kappa_2 = 0.01$ are shown in Figure 7 and Figure 8 for temperature and heat flux respectively. Again, MPCM1 yields fluctuated results for both temperature and heat flux, while the results of MPCM2 are fluctuation free and are very close to the analytical solutions.

[Insert Fig. 7 here]

[Insert Fig. 8 here]

The test problem solved above is actually one-dimensional. To further test MPCM1 and MPCM2, we here consider a two-dimensional problem, as shown in Figure 9. The whole domain is a square with the dimensionless length of 1. The center part of the domain is a square with the dimensionless length of 0.5 and is made of a material ($\kappa_1 = 0.01$) different from that of the outer part ($\kappa_2 = 1$). A regular grid with a total of 1681 (41×41) points is used in the simulation. Shown in Figure 10 and Figure 11 are the temperature profiles along a horizontal line and a vertical line respectively. Results from a finite element method are used for comparison. Again, MPCM2 outperforms MPCM1 in terms of accuracy and smoothness.

[Insert Fig. 9 here]

[Insert Fig. 10 here]

[Insert Fig. 11 here]

5. Conclusions

A truly meshless method based on the WLS approximation and the point collocation approach is presented for the numerical simulation of heat conduction problems in heterogeneous media. The proposed method employs the WLS approximation for points inside homogeneous domains and the double stage WLS approximation for points at interfaces. Besides these, the proper neighbor selection criterion is introduced for the double stage WLS approximation. It is shown that the proposed method is able to obtain accurate and smooth solutions in case of strong heterogeneity. The proposed method can be easily extended to transient problems.

Reference

1. T. Belytschko, Y. Lu, and L. Gu, Element Free Galerkin Methods, *Comput. Mech.*, vol. 37, pp. 229-256, 1992.
2. T. Liszka and J. Orkisz, Finite Difference Method at Arbitrary Irregular Grids and Its Application in Applied Mechanics, *Comput. Struct.*, vol. 11, pp. 83-95, 1979.
3. E. Oñate, S. Idelsohn, O. Zienkiewicz, and R. Taylor, A Finite Point Method in Computational Mechanics: Applications to Convective Transport and Fluid Flow, *Int. J. Numer. Methods Eng.*, vol. 39, pp. 3839-3866, 1996.
4. H. Sadat and C. Prax, Application of the Diffuse Approximation for Solving Fluid Flow and Heat Transfer Problems, *Int. J. Heat Mass Transf.*, vol. 39, pp. 214-218, 1996.
5. E. Oñate, S. Idelsohn, O. Zienkiewicz, and R. Taylor, A Stabilized Finite Point Method for Analysis of Fluid Mechanics Problems, *Comput. Meth. Appl. Mech. Eng.*, vol. 139, pp. 315-346, 1996.
6. R. Löhner, C. Sacco, E. Oñate, and S. Idelsohn, A Finite Point Method for Compressible Flow, *Int. J. Numer. Methods Eng.*, vol. 53, pp. 1765-1779, 2002.
7. E. Oñate, S. Sacco, and C. Idelsohn, A Finite Point Method for Incompressible Flow Problems, *Comput. Visual. Sci.*, vol. 3, pp. 67-75, 2000.

8. J. Fang and A. Parriaux, A Regularized Lagrangian Finite Point Method for the Simulation of Incompressible Viscous Flows, *J. Comput. Phys.*, vol. 227, pp. 8894-8908, 2008.
9. E. Ortega, E. Oñate , and S. Idelsohn, An Improved Finite Point Method for Tridimensional Potential Flows, *Comput. Mech.*, vol. 40, pp. 949-963, 2007.
10. L. Zhang, Y. Rong, H. Shen, and T. Huang, Solidification Modeling in Continuous Casting by Finite Point Method, *J. Mater. Process. Technol.*, vol. 192, pp. 511-517, 2007.
11. E. Oñate, F. Perazzo, and J. Miquel, A Finite Point Method for Elasticity Problems, *Comput. Struct.*, vol. 79, pp. 2151-2163, 2001.
12. S. Tiwari and J. Kuhnert, Modeling of Two-Phase Flows with Surface Tension by Finite Pointset Method (FPM), *J. Comput. Appl. Math.*, vol. 203, pp. 376-386, 2007.
13. S. Tiwari, S. Antonov, D. Hietel, J. Kuhnert, F. Olawsky, and R. Wegener, A Meshfree Method for Simulations of Interactions Between Fluids and Flexible Structures, in M. Griebel and M. Schweitzer (eds.), *Meshfree Methods for Partial Differential Equations III, Vol. 57 of Lecture Notes in Computational Science and Engineering*, pp. 249-264, Springer, Berlin, 2007.
14. H. Sadat, N. Dubus, L. Gbahoué, and T. Sophy, On the Solution of Heterogeneous Heat Conduction Problems by a Diffuse Approximation Meshless Method, *Numer. Heat Transfer B*, vol. 50, pp. 491- 498, 2006.

Figure captions

Fig. 1. Two-dimensional heat conduction in a two-layered composite wall.

Fig. 2. The point distribution used for space discretization.

Fig. 3. The temperature profile for $\kappa_1/\kappa_2 = 0.01$ and $s = 0$. Here MPCM1 (k1) and MPCM1 (k2) mean the thermal conductivities on the interface points are set to k_1 and k_2 respectively. The small figure inside is an enlarged plot for the region $0.5 \leq x \leq 1$.

Fig. 4. The heat flux profile for $\kappa_1/\kappa_2 = 0.01$ and $s = 0$. Here MPCM1 (k1) and MPCM1 (k2) mean the thermal conductivities on the interface points are set to k_1 and k_2 respectively.

Fig. 5. The temperature profile for $\kappa_1/\kappa_2 = 0.01$ and $s = 0$, predicted by MPCM1 using two different grids.

Fig. 6. The heat flux profile for $\kappa_1/\kappa_2 = 0.01$ and $s = 0$, predicted by MPCM1 using two different grids.

Fig. 7. The temperature profile for $\kappa_1/\kappa_2 = 0.01$ and $s = -10$.

Fig. 8. The heat flux profile for $\kappa_1/\kappa_2 = 0.01$ and $s = -10$.

Fig. 9. Two-dimensional heat conduction in a square domain with the center square made of a material different from that of the outer part.

Fig. 10. The temperature profile along the horizontal line at $y = 0.5$ for $\kappa_1/\kappa_2 = 0.01$ and $s = 0$.

Fig. 11. The temperature profile along the vertical line at $x = 0.875$ for $\kappa_1/\kappa_2 = 0.01$ and $s = 0$.

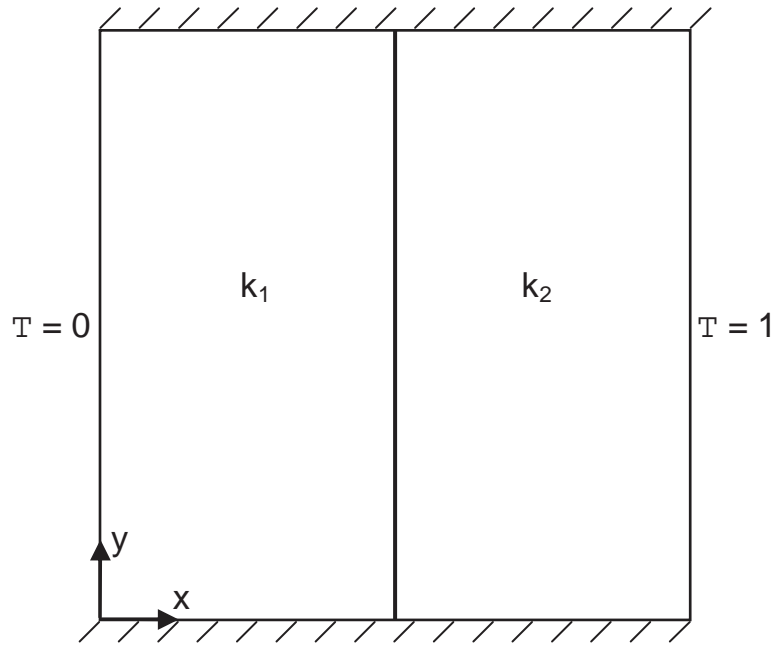


Figure 1 (J. Fang)

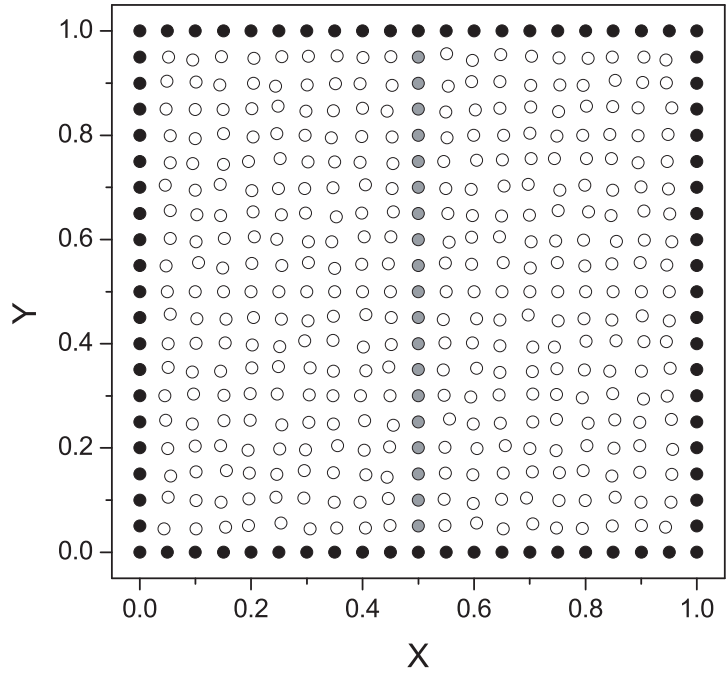


Figure 2 (J. Fang)

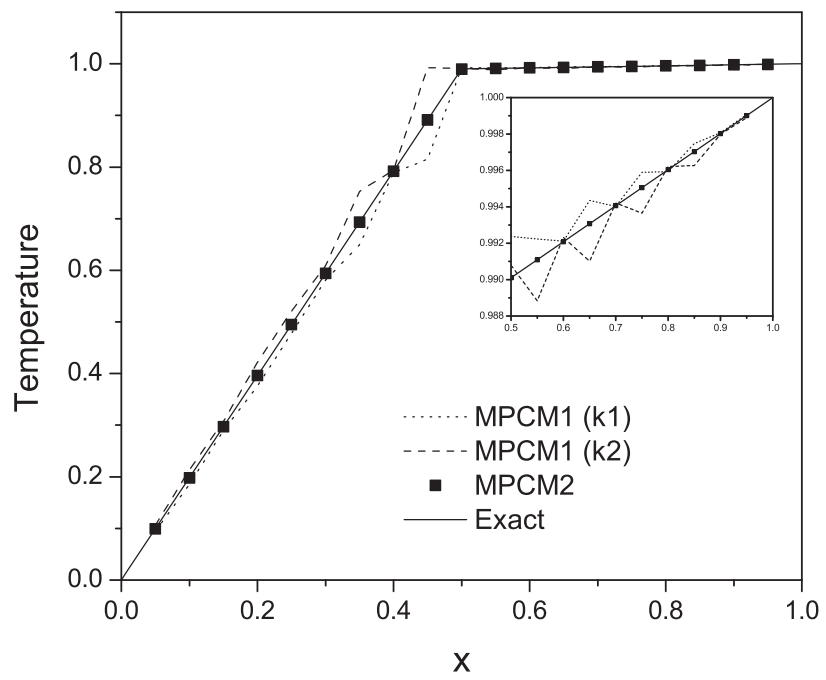


Figure 3 (J. Fang)

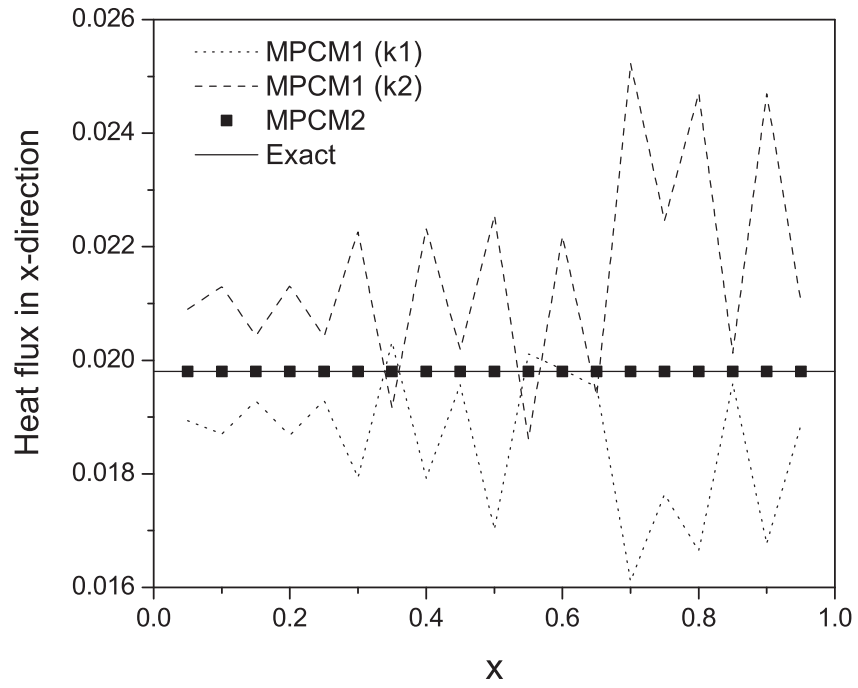


Figure 4 (J. Fang)

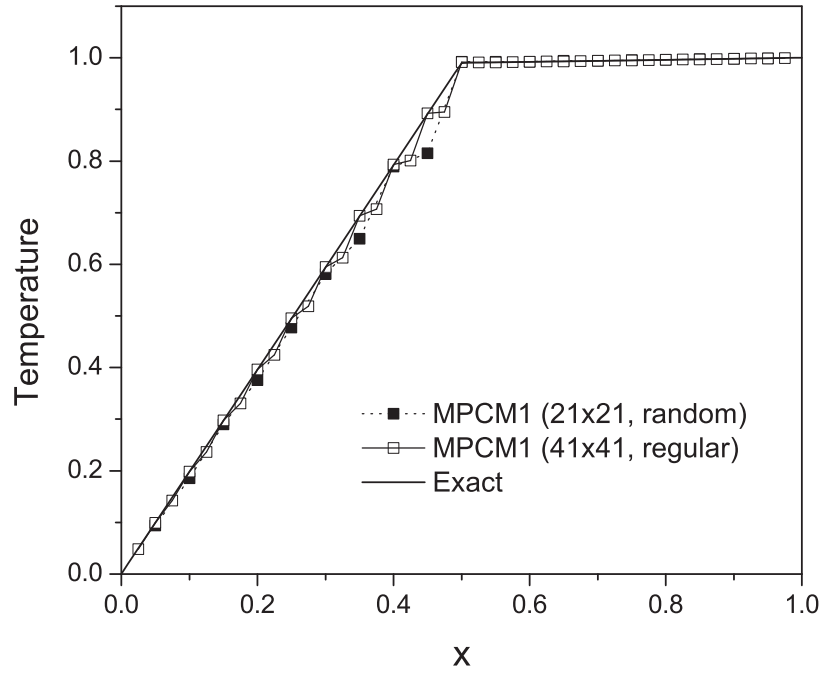


Figure 5 (J. Fang)

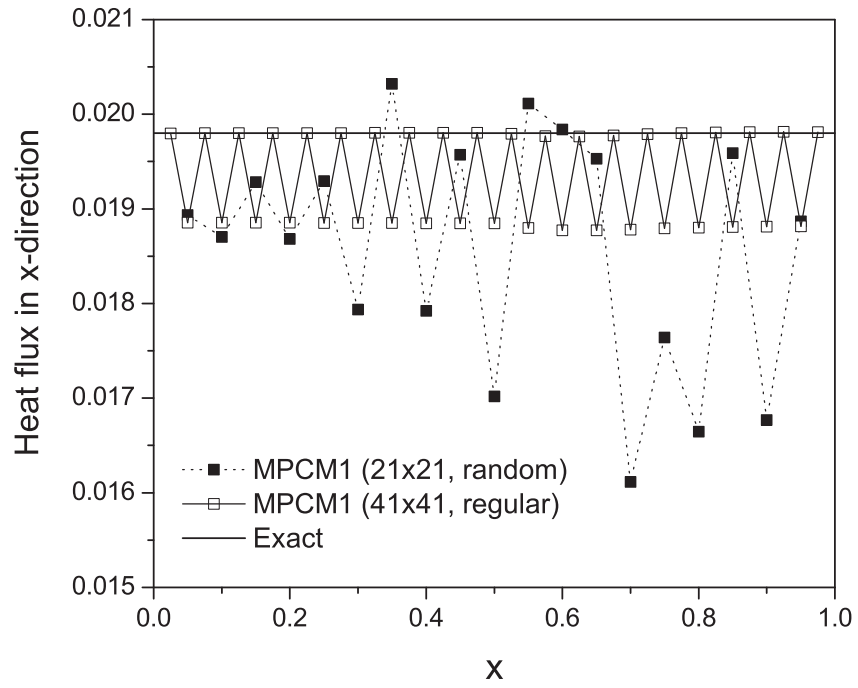


Figure 6 (J. Fang)

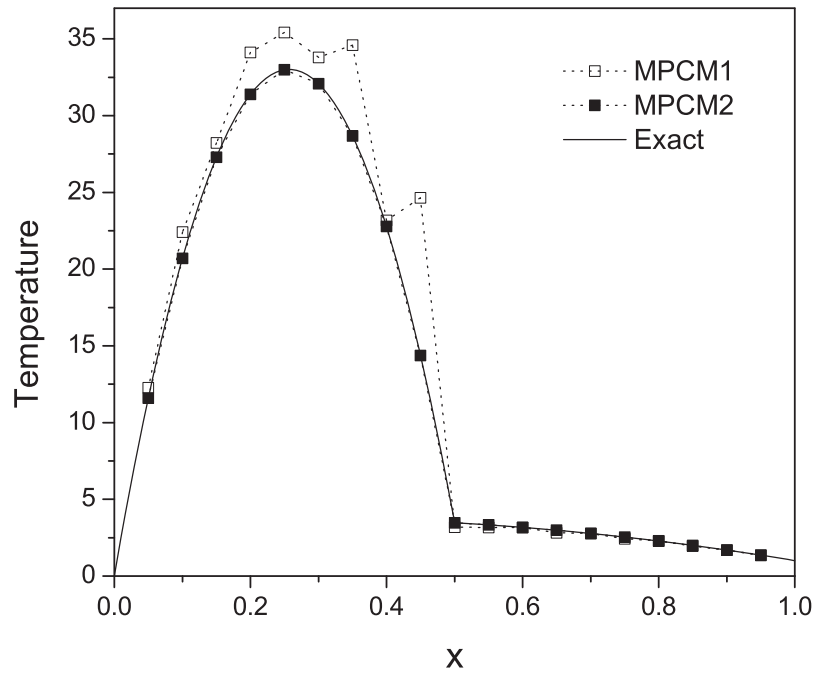


Figure 7 (J. Fang)

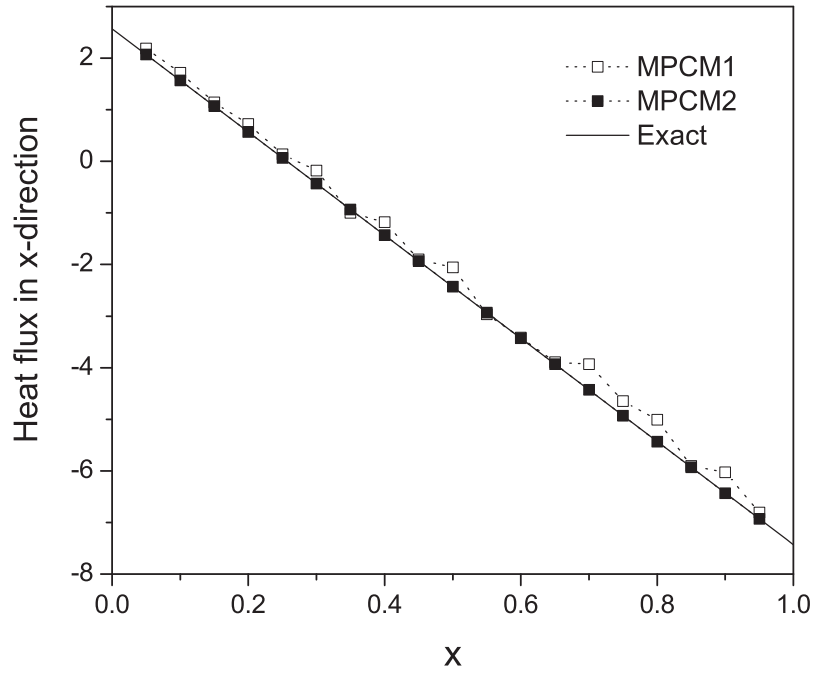


Figure 8 (J. Fang)

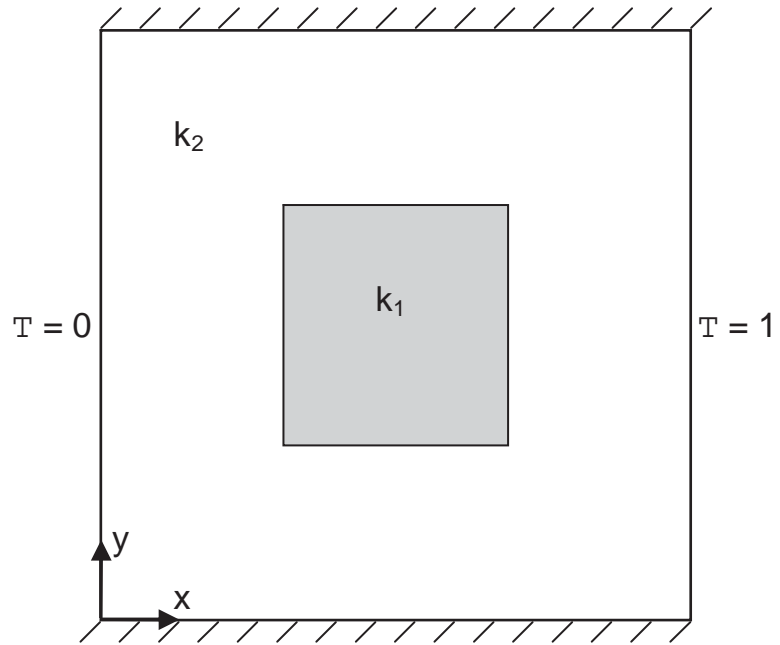


Figure 9 (J. Fang)

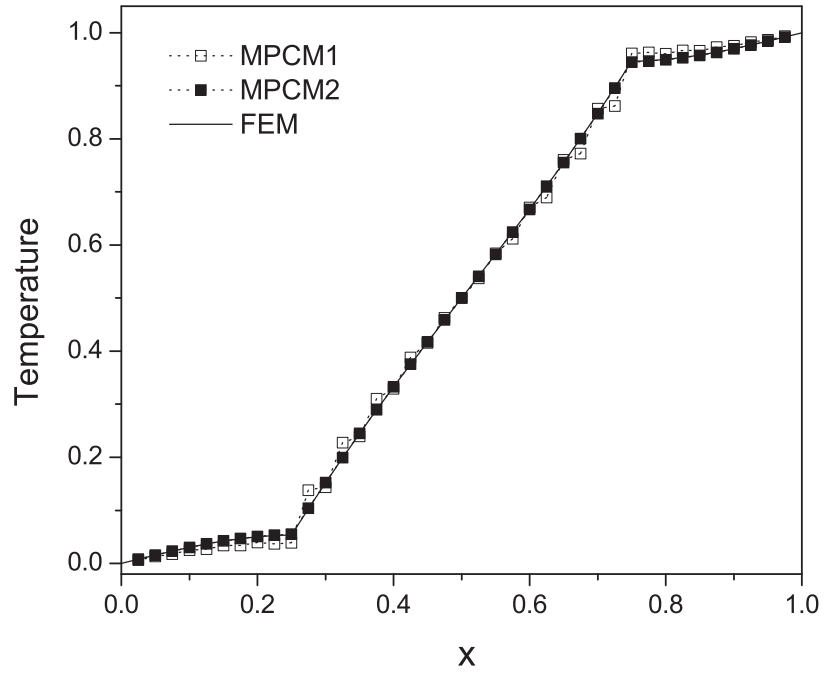


Figure 10 (J. Fang)

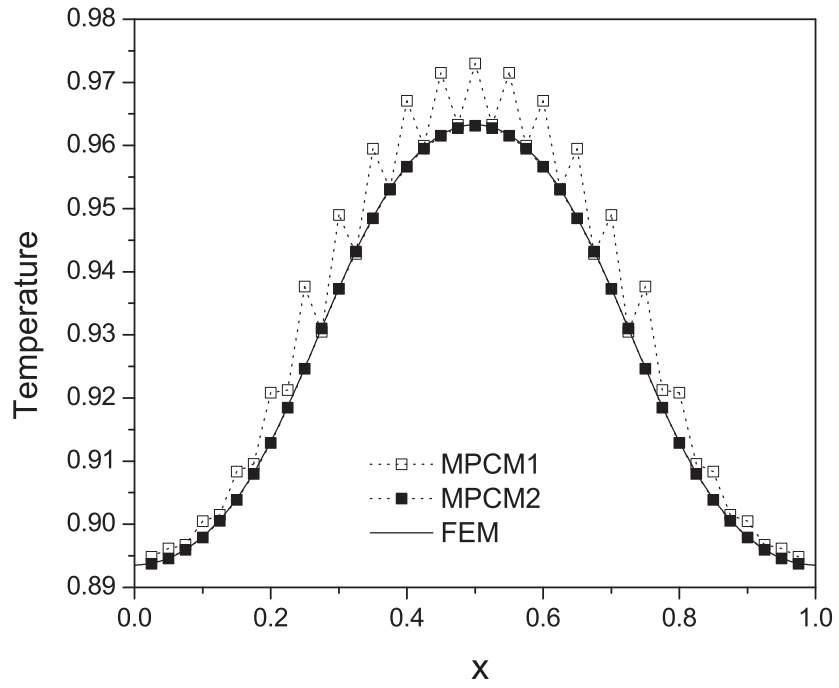


Figure 11 (J. Fang)